Structure of the Photo-catalytically Active Surface of SrTiO3

Manuel Plaza,[†,#,¶] Xin Huang,[†,¶] J. Y. Peter Ko,[†,▽] Mei Shen,[‡] Burton H. Simpson,[‡] Joaquín Rodríguez-López,[‡,¶] Nicole L. Ritzert,[§,⊗] Kendra Letchworth-Weaver,[‖,¶] Deniz Gunceler,[‖] Darrell G. Schlom,[⊥,△] Tomás A. Arias,*[‖] Joel D. Brock,*[†] and Héctor D. Abruña*[§]

[†]School of Applied and Engineering Physics, Cornell University, Ithaca, New York 14853, United States
[‡]Department of Chemistry, University of Illinois at Urbana−Champaign, Urbana, Illinois 61801, United States
[§]Department of Chemistry and Chemical Biology, Cornell University, Ithaca, New York 14853, United States
[‖]Department of Physics, Cornell University, Ithaca, New York 14853, United States
[⊥]Department of Materials Science and Engineering, Cornell University, Ithaca, New York 14853, United States
[△]Kavli Institute at Cornell for Nanoscale Science, Ithaca, New York 14853, United States

S *Supporting Information*

ABSTRACT: A major goal of energy research is to use visible light to cleave water directly, without an applied voltage, into hydrogen and oxygen. Although SrTiO3 requires ultraviolet light, after four decades, it is still the "gold standard" for the photo-catalytic splitting of water. It is chemically robust and can carry out both hydrogen and oxygen evolution reactions without an applied bias. While ultrahigh vacuum surface science techniques have provided useful insights, we still know relatively little about the structure of these electrodes in contact with electrolytes under operating conditions. Here, we report the surface structure evolution of a n-SrTiO3 electrode during water splitting, before and after "training" with an applied positive bias. *Operando* high-energy X-ray reflectivity measurements demonstrate that training the electrode irreversibly reorders the surface. Scanning electrochemical microscopy at open circuit correlates this training with a 3-fold increase of the activity toward the photo-induced water splitting. A novel first-principles joint density functional theory simulation, constrained to the X-ray data via a generalized penalty function, identifies an anatase-like structure as the more active, trained surface.

Figure 1. (a) SrTiO3 unit cell. Crystal structure alternates SrO and TiO2 layers along [001]. (b) Schematic of the experimental setup for *operando* X-ray reflectivity of SrTiO3 during photo-assisted (electro)-chemistry. (c) Tapping-mode AFM image of SrTiO3 after surface preparation. The inset shows the height profile of the shadowed area of the AFM image. Atomic terraces are about 0.5 nm in height and 90 nm in width. (d) Light-chopped linear sweep voltammogram of SrTiO3 in 0.1 M NaOH. The power of light illumination directly on the sample was 15 mW/cm²; scan rate was 20 mV/s.

Wide-band-gap, n-type, metal oxide semiconductors such as SrTiO3, TiO2, and WO3 absorb ultraviolet (UV) light to form photo-generated (electrons and holes) charge carriers, capable of driving redox reactions at the interface with an electrolyte.[1−3] SrTiO3 is a prototypic perovskite structure metal oxide (Figure 1a). The perovskites exhibit a vast range of attractive physicochemical properties, including promising energy conversion activity.[4] Since the initial reports of the UV activity of n-TiO2 and n-SrTiO3 in the 1970s, researchers have pursued a fundamental understanding of the mechanistic and molecular-level phenomena involved in photo-catalysis.[5−11] In particular, SrTiO3 has very attractive photo-catalytic properties. It is highly stable in base, displays high quantum efficiency for the electro-oxidation of water under UV illumination, and performs the light-driven water splitting reaction (i.e., photo-generation of both O2 and H2 from H2O)

under an applied bias,[6,12] at open circuit aided by an auxiliary metal electrode,[6,12] and on free-standing crystals.[7,8,12−15] The fundamental mechanisms underlying surface photo-electro-chemical reactions, however, remain unclear. While the bulk d-band structure can correlate with activity,[4] surface defects and surface structure are critically important, and it is generally difficult to decouple the bulk and surface contributions to observed changes in reactivity.[16−18] Here, we illustrate the critical role that surface structure plays by demonstrating, under

operando conditions, that the electrochemical activation ("training") of n-doped SrTiO$_3$(001) in basic media, by biasing at 0.8 V vs Ag/AgCl for 40 min, induces an irreversible surface reordering that enhances (by 260%) its activity for photocatalytic water splitting.

The *operando* structural characterization of SrTiO$_3$ before and after training was performed using high-energy X-ray reflectivity to measure the specular crystal truncation rod (CTR) during photo-catalytic water splitting.[19,20] Taking advantage of the penetrating power of high energy (30 keV) X-rays, a novel photo-electrochemical cell (Figure 1b), and a large format area detector optimized for hard X-rays, we measured absolute X-ray structure factors. The sub-angstrom sensitivity of CTR to average surface/interface structure allows us to characterize the SrTiO$_3$(001)/electrolyte interface and the bulk-like layers beneath, while maintaining strict control of the electrochemical reaction conditions. Scanning electrochemical microscopy (SECM)[21] was used to follow sequential functional changes (e.g., O$_2$ evolved or adsorbed oxygen-containing intermediates)[22,23] at the surface. Joint density functional theory (JDFT)[24,25] was employed to calculate the electronic structure, geometry, and X-ray structure factors of the SrTiO$_3$ surface in the presence of a liquid description with atomic-scale structure. A detailed description of each of these methods is given in the Supporting Information (SI).

We carefully prepared the n-SrTiO$_3$ electrode to ensure an atomically smooth surface with well-defined doping and benchmarked its UV light-induced water-splitting activity to optimize our experimental design. As shown in Figure 1c, chemical etching produced atomically flat terraces on the SrTiO$_3$(001) surface. Precisely controlled vacuum annealing, followed by a thermal quench, fixed the bulk oxygen vacancy concentration and concomitant carrier density to $n_D \approx 1 \times 10^{17}$ cm^{-3}, producing samples with a clear photo-current signal in 0.1 M NaOH electrolyte under illumination with a 200 W Hg/Xe lamp. Figure 1d shows a typical photo-current vs applied potential profile under chopped illumination, where the anodic photo-current corresponds to the electrochemical oxidation of water to form O$_2$. Large photo-currents occur only under UV irradiation. Monochromatic UV light, centered at $\lambda = 390 \pm 20$ nm ($\sim$3.2 eV), was used in subsequent experiments to control the illumination conditions precisely.

Figure 2a shows the measured X-ray structure factors, $|F|^2$, of n-doped SrTiO$_3$(001) in air and in electrolyte (both before and after training). The data from samples in air are consistent with previous reports in the literature,[26] and the line-shape is the same for doped and undoped samples. Nonlinear least-squares fits of $|F|^2$ to atomic models (solid blue line in Figure 2a) suggest that the structure represents a relaxation of the well-known TiO$_2$ double-layer model.[27,28] Immersing the doped substrates in 0.1 M NaOH, however, dramatically alters $|F|^2$ and the resulting (untrained) surface structure is stable in electrolyte under UV illumination. The same structural evolution also occurs in 0.1 M CsOH, suggesting that the countercation does not play a role in these structural changes. This structural evolution does not occur for undoped samples in either 0.1 M NaOH or 0.1 M H$_2$SO$_4$. Reports in the literature previously established that photo-assisted water splitting, at open circuit, is negligible for n-SrTiO$_3$ in H$_2$SO$_4$, but readily observed in basic medium.[13] Figure 2b schematically illustrates the dependence of the structural evolution upon doping and choice of electrolyte.
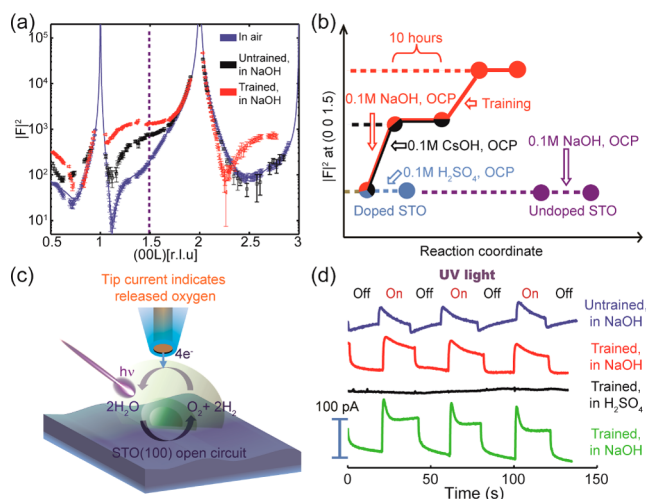
Figure 2. (a) Structure factor of 00L CTR of SrTiO$_3$ in air (blue), in 0.1 M NaOH at open circuit before (black) and after (red) training. "r.l.u" stands for reciprocal lattice units. Blue solid line is the best nonlinear least-squares fits to the CTR of SrTiO$_3$ in air, using the TiO$_2$ double-layer model. (b) Map to the evolution of $|F|^2$ at (0 0 1.5) of samples in different electrolytes: red, doped SrTiO$_3$ in 0.1 M NaOH; black, doped SrTiO$_3$ in 0.1 M CsOH; blue, doped SrTiO$_3$ in 0.1 M H$_2$SO$_4$; and purple, undoped SrTiO$_3$ in 0.1 M NaOH. (c) SECM in O$_2$ substrate collection mode. The Hg/Au amalgam tip detects the oxygen produced by the water splitting reaction at the SrTiO$_3$ electrode at open circuit. (d) SECM collection with UV light on/off: blue, in 0.1 M NaOH before training; red, after training (biasing to 0.8 V vs Ag/AgCl for 40 min); black, upon immersion in 0.1 M H$_2$SO$_4$; and green, after returning to 0.1 M NaOH. The oxygen generation rate is proportional to the current, 100 pA $\sim$ 200 mol h^{-1} m^{-2} (see Figure S19).

These experimental studies of the stoichiometry and atomic structure of the untrained surface offer an excellent starting point for interpretation by JDFT calculations. Other state-of-the-art *ab initio* techniques for the study of electrochemical interfaces either require computationally prohibitive molecular dynamics to sample the liquid structure, or they consider the surface in vacuum or with only a single frozen layer of water. Our JDFT calculations efficiently include the atomically detailed structure of a thermodynamically sampled liquid by construction.[25] Because JDFT provides full access to the electron density of both the solid surface and the contacting liquid, we calculate $|F|^2$ and compare it directly with experiment. Figure 3b displays the best JDFT candidate structure for untrained SrTiO$_3$ immersed in 0.1 M NaOH, a relaxed 1×1 double-TiO$_2$-terminated structure. The black curve in Figure 3a shows that the JDFT calculated $|F|^2$ agrees extremely well with experiment *with no adjustable parameters*, thereby demonstrating the power of the JDFT approach. The JDFT structure describes the X-ray data much more accurately than the 2×1 reconstruction that has the minimum free energy in air or an *ab initio* calculation with a single layer of water molecules adsorbed on the surface (see Figure S13).

As shown in Figure 2a, when an electrode is trained (biased to +0.8 V vs Ag/AgCl) during UV illumination, the surface evolves to a new stable structure. Trained electrodes exhibit a significant enhancement of $|F|^2$ between the 001 and 002 peaks that is independent of the electrode potential. This enhancement of $|F|^2$ may be characterized by defining a reaction coordinate midway between the two peaks (dotted line in Figure 2a). Figure 2b summarizes the dependence of this
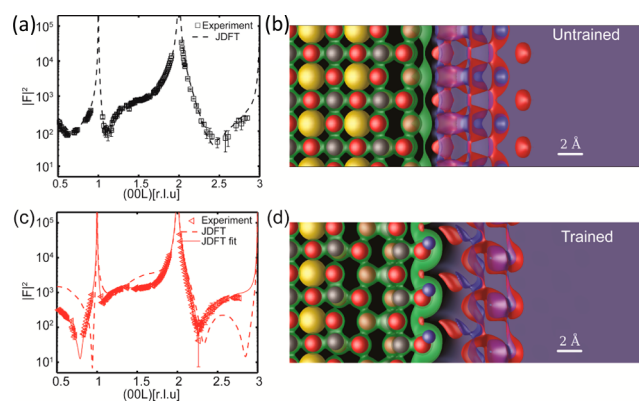
Figure 3. (a) Structure factor of 00L CTR of untrained $SrTiO_3$ in 0.1 M NaOH. Black squares are experimental data. Black dashed line is the structure factor calculated from the JDFT structure, with no adjustable parameters. (b) JDFT structure for the untrained $SrTiO_3$ surface. (c) Structure factor of 00L CTR of trained $SrTiO_3$ in 0.1 M NaOH. Red triangles are experimental data. Red dashed line is from JDFT structure, with no adjustable parameters. Red solid line is a guided fit constrained to the JDFT structure with a penalty function. (d) JDFT structure for the trained $SrTiO_3$ surface before fitting. Yellow spheres are strontium, red are oxygen, blue are hydrogen, and silver are titanium atoms. Green, red, and blue density contours represent electron, oxygen, and hydrogen density, respectively, as described in the SI.

enhancement upon doping, choice of electrolyte, and history of applied bias. SECM measurements (Figure 2c) using a selective O_2 microelectrode, under thoroughly deoxygenated conditions and UV light chopping, demonstrate a large increase in the photo-catalytic activity on trained substrates.[21] SECM can measure the minute changes in O_2 evolution with sufficiently high temporal resolution to characterize, *in situ*, the reactivity of the open circuit $SrTiO_3$ surface just before and after training. Although the activity at open circuit represents only a small fraction of the activity at 0.8 V vs Ag/AgCl, the impact of the subtle surface change on the activity at open circuit is profound. The activity of the trained $SrTiO_3$ surface is 2.6 ± 0.9 times larger than that of the untrained surface.[30] (Figure 2d) The same substrates, even after training, were not active toward photo-catalytic water splitting in acidic medium, but recovered the enhanced activity if returned back to 0.1 M NaOH (Figures 2d and S19). The training-induced structural change survives removal from the electrochemical cell and thorough rinsing with water. Because, at open circuit, transport is not aided by an external field, bulk carrier recombination limits the quantum efficiency. Nevertheless, our results clearly demonstrate the correlation between the structural change, in only the topmost atomic layers, and the enhanced reactivity.

We explored two possible explanations for the training-induced structural change: (1) the formation of a photo-generated surface intermediate O(H) ad-layer, and (2) a change in crystal structure of the surface. Pursuing the ad-layer hypothesis, we performed surface interrogation SECM,[22,23] which demonstrated that a limiting coverage, consistent with one equivalent of reactive O (or two OH) per unit cell of $SrTiO_3$, is reached at positive potentials (see SI). However, nonlinear least-squares fits of the X-ray data to atomic models indicated that the addition of an O(H) ad-layer alone cannot explain the observed change of $|F|^2$, particularly between the 001 and 002 peaks.

To explore the structure change hypothesis, we relaxed multiple (~100) surface stoichiometries and geometries within JDFT and found that the only likely candidate for the trained surface is an oxygen-deficient, biaxially strained, anatase-like structure, as shown in Figure 3d. Since anatase is also a catalyst for photo-assisted water splitting, it is perhaps not surprising that the trained surface is associated with enhanced reactivity. At least one layer of Sr atoms has been removed, leaving a triple TiO_2 termination and explaining the observed irreversibility of the training. This predicted reduction in surface concentration of Sr is in good agreement with the XPS *ex situ* experiment we performed. This candidate for the trained structure has the Ti-stacking of anatase rather than $SrTiO_3$, and it is oxygen deficient at the surface. In fact, a similarly stacked triple-layer TiO_2 terminated surface has been previously observed after ultrahigh vacuum annealing by combined XPS-STM studies.[29] This similar ex situ structure has been shown to exhibit a mid-band-gap state which could provide further explanation for the observed increased activity for photo-electrochemical water-splitting.

The JDFT calculation which agrees best with the X-ray data for the trained surface has the stoichiometry of Ti_2O_2 at the surface with a capping hydroxide layer. However, there is still significant discrepancy between the JDFT calculation with no adjustable parameters and the experimental structure factor (see the dotted line in Figure 3c).

A JDFT-guided nonlinear least-squares fit to the experimental structure factor allows the atoms to move away from their minimum energy positions to consider the effect of nonequilibrium or thermal processes, and to develop partial occupancies to account for missing surface atoms and other disorder. Adding a generalized penalty function to the traditional chi-squared fit, allows exploration of other surface configurations with energies within approximately kT (room temperature) per atom of the JDFT minimum energy. The solid red curve in Figure 3c applies this JDFT-guided fit procedure to the above-described, minimum energy structure. This particular fit prevents atoms from moving more than 0.22 Å from their JDFT positions and has the excitation energy of less than 2 kT per fit atom. The partial occupancy of Ti atoms in this fit suggests a (still O-deficient) surface stoichiometry between Ti_2O_2 and TiO_2. The agreement between the JDFT-guided and experimental structure factors is now excellent, providing convincing evidence that the trained $SrTiO_3$ surface must exhibit an anatase-related structure (as in Figure 3d).

The identification of a highly reactive, anatase-related termination for the $SrTiO_3$ surface after training could have significant impact upon the field of photo-catalysis. Going forward, establishing the structural and photo-catalytic differences between anatase and the anatase-related surface of $SrTiO_3(001)$ may provide insights into ways to engineer improved photo-catalysts. Unlike $SrTiO_3$, anatase has the disadvantage of requiring an applied bias to photo-generate both O_2 and H_2 from H_2O. However, anatase has a smaller band gap than $SrTiO_3$, enabling it to capture more of the solar spectrum. The similarity in the active surface of these established photo-catalysts suggests a separation of roles between the surface and the bulk of a designer photo-catalyst. For example, combining an anatase-related surface (to provide chemical stability and high catalytic activity) with an underlying host that is better matched to the solar spectrum and can impose optimal biaxial strain on the surface ($SrTiO_3$ imposes a 3.2% biaxial tensile strain) is a clear strategy for the future.

This work illustrates the critical role that history-dependent surface structure plays in the photo-catalytic water-splitting activity of $SrTiO_3$. Combining and integrating information from *operando* X-ray surface-sensitive techniques, electrochemical and functional characterization methods, and JDFT calculations, we demonstrate that training the $SrTiO_3$ electrode changes the surface structure from a double layer TiO_2 termination to an oxygen-deficient biaxially strained anatase-like structure, and concurrently triples the photo-activity. The profound dependence of electrode structure and reactivity upon the training by an applied bias has broad implications beyond just photo-catalysis. The insights gained in this work are highly relevant to the design of surface chemical modifications for applications such as pollutant remediation and functional coatings, where surface reactivity under zero applied bias is key. Furthermore, the synergistic combination of *in situ* measurement techniques with theory opens a promising path toward fundamental mechanistic understanding of surface reactivity in electrolyte media.

ASSOCIATED CONTENT

Ⓢ Supporting Information

The Supporting Information is available free of charge on the ACS Publications website at DOI: 10.1021/jacs.6b03338.

> Methodology of CTR, sample preparation, photo-electrochemical characterization, details of in situ CTR measurements and interpretation, details of JDFT calculation, surface reactivity characterization with SECM and XPS, Figures S1−S20, and Tables S1−S3 (PDF)

AUTHOR INFORMATION

Corresponding Authors

*taa2@cornell.edu
*jdb20@cornell.edu
*hda1@cornell.edu

Present Addresses

[#]M.P.: Departamento de Física de la Materia Condensada, Universidad Autónoma de Madrid, Ciudad Universitaria de Cantoblanco, 28049, Madrid, Spain

[∇]J.Y.P.K.: Cornell High Energy Synchrotron Source, Cornell University, Ithaca, NY 14853, USA

[⊗]N.L.R.: Material Measurement Laboratory, National Institute of Standards and Technology, Gaithersburg, MD 20899, USA

[◇]K.L.-W.: Center for Nanoscale Materials, Argonne National Laboratory, Lemont, IL 60439, USA

Author Contributions

[¶]M.P., X.H., J.R.L., and K.L.W. contributed equally.

Notes

The authors declare no competing financial interest.

REFERENCES

(1) Nozik, A. J.; Memming, R. *J. Phys. Chem.* **1996**, *100*, 13061.
(2) Bard, A. J. *Science* **1980**, *207*, 139.
(3) Tan, M. X.; Laibinis, P. E.; Nguyen, S. T.; Kesselman, J. M.; Stanton, C. E.; Lewis, N. S. *Prog. Inorg. Chem.* **1994**, *41*, 21.
(4) Suntivich, J.; May, K. J.; Gasteiger, H. A.; Goodenough, J. B.; Shao-Horn, Y. *Science* **2011**, *334*, 1383.
(5) Fujishima, A.; Honda, K. *Nature* **1972**, *238*, 37.
(6) Wrighton, M. S.; Ellis, A. B.; Wolczanski, P. T.; Morse, D. L.; Abrahamson, H. B.; Ginley, D. S. *J. Am. Chem. Soc.* **1976**, *98*, 2774.
(7) Wagner, F. T.; Somorjai, G. A. *Nature* **1980**, *285*, 559.
(8) Carr, R. G.; Somorjai, G. A. *Nature* **1981**, *290*, 576.
(9) Gratzel, M. *Nature* **2001**, *414*, 338.
(10) Khaselev, O.; Turner, J. A. *Science* **1998**, *280*, 425.
(11) Bolton, J. R.; Strickler, S. J.; Connolly, J. S. *Nature* **1985**, *316*, 495.
(12) Mavroides, J. G.; Kafalas, J. A.; Kolesar, D. F. *Appl. Phys. Lett.* **1976**, *28*, 241.
(13) Wagner, F. T.; Ferrer, S.; Somorjai, G. A. *ACS Symp. Ser.* **1981**, *146*, 159.
(14) Domen, K.; Naito, S.; Onishi, T.; Tamaru, K. *Chem. Phys. Lett.* **1982**, *92*, 433.
(15) Kraeutler, B.; Bard, A. J. *J. Am. Chem. Soc.* **1978**, *100*, 5985.
(16) Gerischer, H. In *Photoeffects at Semiconductor-Electrolyte Interfaces*; Nozik, A., Ed.; American Chemical Society: Washington, DC, 1981; p 16.
(17) Ong, W.-J.; Tan, L.-L.; Chai, S.-P.; Yong, S.-T.; Mohamed, A. R. *ChemSusChem* **2014**, *7*, 690.
(18) Nakamura, R.; Ohashi, N.; Imanishi, A.; Osawa, T.; Matsumoto, Y.; Koinuma, H.; Nakato, Y. *J. Phys. Chem. B* **2005**, *109*, 1648.
(19) Robinson, I. K. *Phys. Rev. B* **1986**, *33*, 3830.
(20) Robinson, I. K.; Tweet, D. J. *Rep. Prog. Phys.* **1992**, *55*, 599.
(21) Rodríguez-López, J.; Zoski, C. G.; Bard, A. J. In *Scanning Electrochemical Microscopy*, 2nd ed.; Bard, A. J., Mirkin, M. V., Eds.; CRC Press: Boca Raton, FL, 2012.
(22) Rodriguez-Lopez, J.; Minguzzi, A.; Bard, A. J. *J. Phys. Chem. C* **2010**, *114*, 18645.
(23) Zigah, D.; Rodriguez-Lopez, J.; Bard, A. J. *Phys. Chem. Chem. Phys.* **2012**, *14*, 12764.
(24) Petrosyan, S. A.; Briere, J. F.; Roundy, D.; Arias, T. A. *Phys. Rev. B* **2007**, *75*, 205105.
(25) Sundararaman, R.; Arias, T. A. *Comput. Phys. Commun.* **2014**, *185*, 818.
(26) Kazimirov, A.; Goodner, D.; Bedzyk, M.; Bai, J.; Hubbard, C. *Surf. Sci.* **2001**, *492*, L711.
(27) Herger, R.; Willmott, P.; Bunk, O.; Schlepütz, C.; Patterson, B.; Delley, B. *Phys. Rev. Lett.* **2007**, *98*, 076102.
(28) Erdman, N.; Poeppelmeier, K. R.; Asta, M.; Warschkow, O.; Ellis, D. E.; Marks, L. D. *Nature* **2002**, *419*, 55.
(29) Marshall, M. S. J.; Becerra-Toledo, A. E.; Payne, D. J.; Egdell, R. G.; Marks, L. D.; Castell, M. R. *Phys. Rev. B* **2012**, *86*, 125416.
(30) Training increases the relative quantum efficiency (ratio of the efficiency at open circuit to the efficiency at 0.8 V vs Ag/AgCl) from 0.8% to 2.1%. These numbers are from measurements on five samples and at least two sites on each.